Atomic Force Microscopy

DOI: 10.1002/anie.201201890

Direct Visualization of the Movement of a Single T7 RNA Polymerase and Transcription on a DNA Nanostructure**

Masayuki Endo, Koichi Tatsumi, Kosuke Terushima, Yousuke Katsuda, Kumi Hidaka, Yoshie Harada, and Hiroshi Sugiyama**

Direct visualization of intact enzymes interacting with DNA is one of the ultimate methods for investigating the mechanical behavior of enzymes and understanding biological processes.[1,2] Transcription by RNA polymerase (RNAP) is one of the most important biological processes. Transcription involves a series of RNAP behaviors, including binding to double-stranded DNA (dsDNA), sliding along the dsDNA, RNA synthesis, and dissociation from the dsDNA. The molecular behavior of RNA polymerase during transcription has been investigated by atomic force microscopy (AFM)[3–6] and fluorescence microscopy.[7–10] Recently, high-speed AFM has enabled visualization the movements of single molecules at nanoscale resolution in real time.[11–14] For consistent imaging of single-molecule enzymatic reactions, an observation platform is required. The DNA origami self-assembly system, which enables specific DNA strands to be placed onto a self-assembled scaffold, can be used to design a wide variety of nanostructures.[15–20] We recently developed one such DNA scaffold, the "DNA frame", which incorporates dsDNAs of various lengths into the scaffold at specific positions and enables visualization of single-enzyme movements and reactions.[21–23]

In this study, we directly observed transcription using an AFM-based single-molecule system. We prepared a nanoscale observation platform using the DNA origami method (Figure 1a). A template dsDNA (1000 bp) containing the T7 promoter was attached at two specific positions on this platform (Figure 1b). Using the DNA origami nanostructure as an observation platform, we directly observed the molecular movement of a single RNAP, including its DNA binding, sliding, RNA synthesis, and dissociation, using high-speed AFM and analyzed the mechanical behavior of RNAP during the transcription process.

For placement of the template dsDNA, we designed a rectangular DNA origami scaffold (1150 bp × 6 duplexes) with a 10.5 bp helical pitch (63 bp per six turns) to avoid super-helical structures.[19] The two positions for the anchoring of the template dsDNA were located at different distances from the ends of the DNA scaffold, so that the orientation of the template dsDNA could be easily determined. For assembly of the DNA origami platform, M13 mp18 single-stranded DNA and complementary DNA strands (staple strands) were annealed in a buffer containing tris-HCl buffer (pH 7.6), EDTA, and Mg^{2+} from 85 °C to 15 °C at a rate of $-1.0\,^{\circ}C\,min^{-1}$ (Supporting Information, Figure S1).[21–23] A PCR-amplified template dsDNA **3** was incorporated between the connection sites A and B in the DNA scaffold (Figure 1c) using corresponding staple strands attached to its ends. In this case, the staple strands at the connection sites were removed, and template dsDNA **3** was attached to the platform **2** by annealing from 50 °C to 15 °C at a rate of $-0.05\,^{\circ}C\,min^{-1}$. The template dsDNA attached to the DNA platform **1** was purified by gel electrophoresis, and the target structure was confirmed by AFM (Figure S2).

Purified **1** was observed in the tris-buffer solution using high-speed AFM. The high-speed AFM system used here enables successive acquisition of one AFM image per second.[11,12] From the successive AFM images, we found that the DNA scaffold was tightly fixed on the mica surface, on the other hand, the template dsDNA was seen as a flexible chain (Figure 2 and Movie S1). Most of the dsDNA chain could be visualized by high-speed AFM, showing that the template dsDNA was connected to the DNA nanoplatform at two positions (Figure 2b and Figure S3). However, the dsDNA chain seemed to widely and randomly contact the mica surface because of the weak charge interaction between the phosphate backbone and the magnesium ion/passivated mica surface. From the AFM images, it appeared that the template dsDNA laid down on the mica surface with both ends fixed to the scaffold (Figure 2b and Figure S3), resulting in restriction of the movement of the dsDNA. The middle area of the dsDNA moved much more than both ends (Figure 2b). The length of the template dsDNA was measured to be 362.0 ± 8.4 nm ($n = 28$ images), which is stretched 6.5% longer than the expected length of the 1000 bp dsDNA (340 nm).

[*] Dr. M. Endo, Prof. Y. Harada, Prof. H. Sugiyama
Institute for Integrated Cell-Material Sciences (WPI-iCeMS)
Kyoto University
Yoshida-ushinomiyacho, Sakyo-ku, Kyoto 606-8501 (Japan)
E-mail: endo@kuchem.kyoto-u.ac.jp
hs@kuchem.kyoto-u.ac.jp
K. Tatsumi, K. Terushima, Y. Katsuda, K. Hidaka, Prof. H. Sugiyama
Department of Chemistry, Graduate School of Science
Kyoto University
Kitashirakawa-oiwakecho, Sakyo-ku, Kyoto 606-8502 (Japan)
Dr. M. Endo, Prof. H. Sugiyama
CREST, Japan Science and Technology Corporation (JST)
Sanbancho, Chiyoda-ku, Tokyo 102-0075 (Japan)

[**] This work was supported by Core Research for Evolutional Science and Technology (CREST) of JST and Grant-in-Aid for Scientific Research from MEXT (Japan). Financial support from Sumitomo foundation and Iketani Science and Technology Foundation to M.E. is also acknowledged.

Supporting information for this article (experimental details) is available on the WWW under http://dx.doi.org/10.1002/anie.201201890.

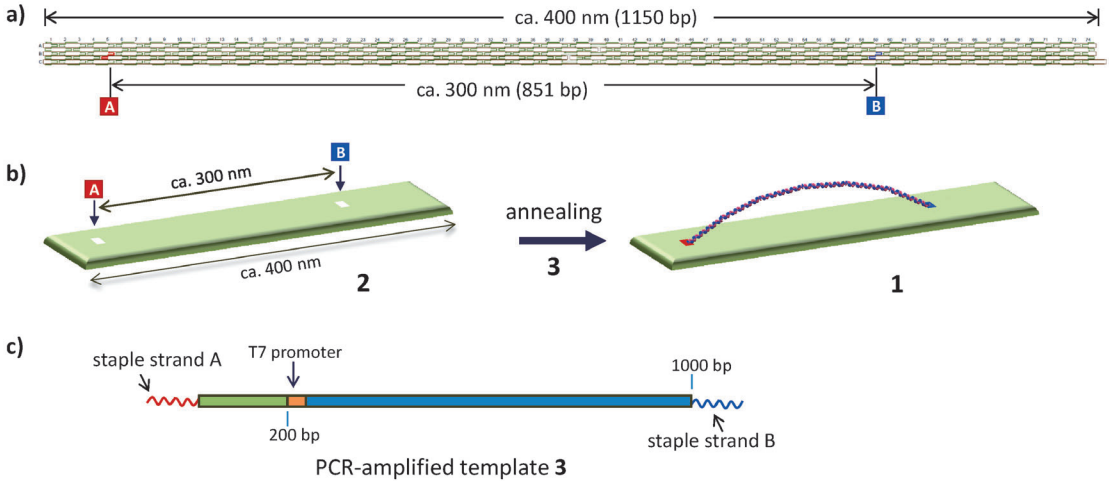

Figure 1. a) Scheme of the DNA origami nanoplatform. Sites A and B show the positions where the template dsDNA is anchored. b) Method for attaching a template dsDNA **3** onto the platform. The DNA nanoplatform **2** was prepared with the staple strands for sites A and B removed. c) A PCR-amplified template dsDNA **3** containing a T7 promoter region and two ssDNA linkers for attachment to platform **2** at sites A and B by annealing.

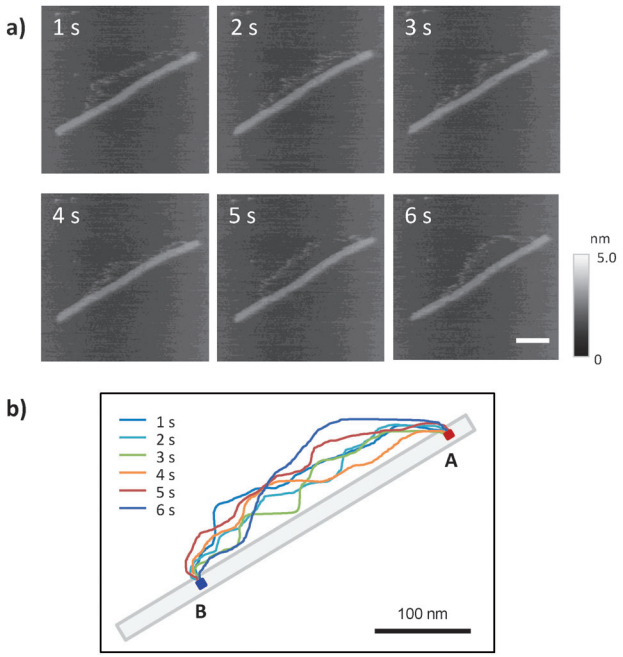

Figure 2. a) High-speed AFM images of the purified template dsDNA attached to the DNA nanoplatform **1**. Images were acquired at 1 image s^{-1}. Scale bar = 100 nm. b) Overlay of the shapes of the template dsDNA chain in the successive AFM images at the various time points. An illustrated DNA nanoplatform and the connection sites A and B are also shown.

We next examined the binding of RNAP to the template dsDNA on the scaffold. To record the movement of the polymerase, RNAP was added to the nanoplatform adsorbed onto the mica surface. Successive images of the sliding of RNAP on the template dsDNA were obtained using high-speed AFM (Figure 3a and Figure S2, and Movie S2). RNAPs that slid along the template dsDNA were easily distinguished from RNAPs that were attached to the mica, as the latter never moved. In addition, the transcribing RNAP is evident as a bright spot because the total height of RNAP bound to dsDNA is higher than that of the RNAP alone. From analysis of the shape of the template dsDNA and the position of RNAP along it (Figure 3b), RNAP bound and moved along the area where the template dsDNA was also mobile. This indicates that RNAP sliding may require partial separation of the dsDNA from the mica surface. In Figure 3c, the positions of RNAP on the template dsDNA are plotted ($n = 46$), and the distribution of the RNAP positions is summarized (Figure 3c). RNAP moved both directions along the dsDNA, however, the statistical distribution shows the average position of the RNAP around the middle of the template dsDNA. This result suggests that mobility of the template dsDNA is needed for RNAP sliding. The one-dimensional diffusion coefficient ($D = <\Delta l^2>/2t$, where Δl is the change of RNAP position along the length of the dsDNA during a time t) obtained from the analysis of the AFM images was $5.1 \pm 0.7 \times 10^{-12}$ $cm^2 s^{-1}$, which is similar to the result of a reported AFM study.[5] Although sliding was imaged directly on the mica surface, the sliding would be affected by contact of the dsDNA with the mica, resulting in a lower one-dimensional diffusion constant for RNAP sliding as compared with the measurement in solution using the fluorescence microscopy.[9]

Next, we examined in vitro transcription using the dsDNA attached to the DNA origami platform **1**. In vitro transcription was carried out in a solution containing **1**, T7 RNAP, and NTPs at 42 °C for 2 h. The transcription mixtures were analyzed using agarose gel electrophoresis (Figure 4a). RNA transcript made from unbound dsDNA was shown (lane 2), and the position of this band was the same as the RNA produced from the dsDNA attached to the nanoplatform **1** (lane 3). This shows that normal transcription occurred even when the template dsDNA was attached to the DNA origami platform at both ends.

We then examined RNA synthesis from **1** on the mica surface. Previous studies showed the difficulty in making

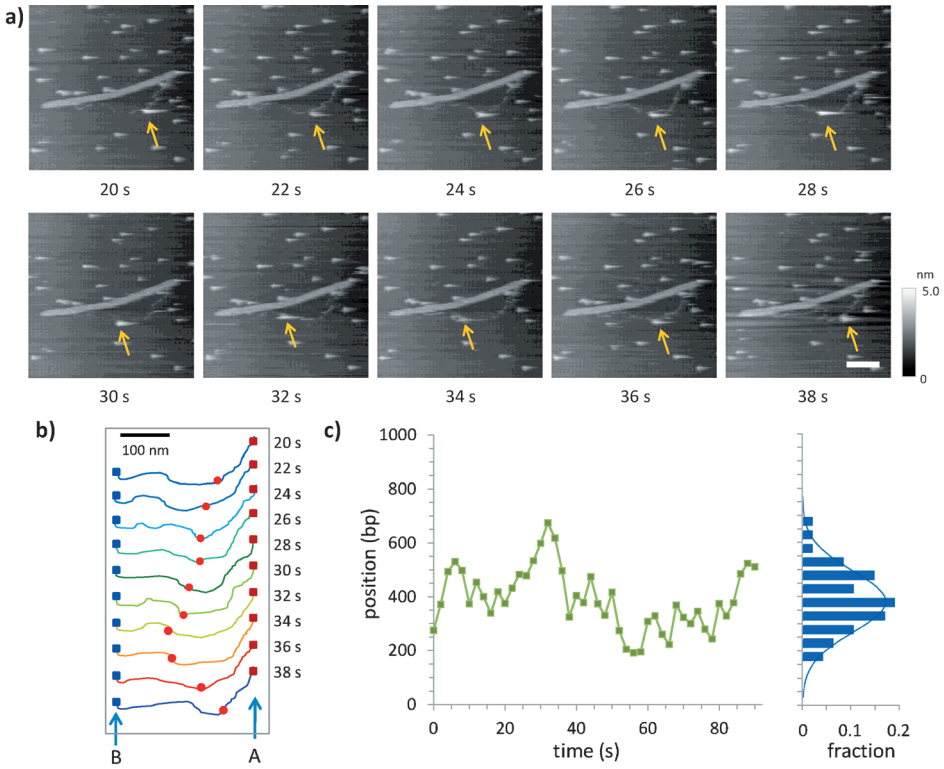

Figure 3. a) High-speed AFM images of RNAP sliding on the template dsDNA attached to the platform. Arrows = position of RNAP. Scanning speed = 0.5 images s^{-1}. Scale bar = 100 nm. b) Shapes of the dsDNA chain and the positions of RNAP (red circle). Rectangles represent the position of sites A (red) and B (purple) on the DNA nanoplatform. c) Left: position of RNAP during sliding on the template dsDNA. Right: distribution of the RNAP positions. Data are fitted to a normal distribution (blue line).

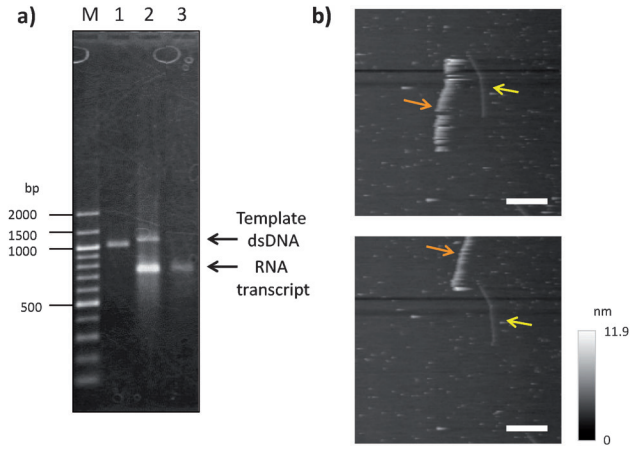

Figure 4. In vitro transcription on the DNA nanoplatform in solution and on the mica surface. a) In vitro transcription in solution. Lane 1: template dsDNA. Lane 2: transcription using unbound template dsDNA. Lane 3: transcription using the purified template dsDNA bound to the nanoplatform. b) In vitro transcription on the mica surface. AFM images of biotinylated RNA transcript (orange arrow) partially labeled with streptavidin. Yellow arrow = template dsDNA on the nanoplatform. Scale bar = 200 nm.

direct observations of transcribed RNA on mica using AFM.[5] For visualization, we employed biotinylated UTP to label the RNA transcript with streptavidin (Figure S5). After attachment of **1** to the mica, RNAP was added in the presence of ATP, CTP, GTP, and biotinylated UTP. Then the mica surface was washed to remove excess NTPs, and the reaction products on the surface were labeled with streptavidin. We observed long streptavidin labeled chains on the mica surface, which moved flexibly (Figure 4b and Figure S6). In contrast, when GTP was absent, no streptavidin labeling was found on the mica surface. These results show that transcribed RNA can be visualized on the mica surface and confirmed that transcription occurred with the template dsDNA/platform fixed to the mica surface.

We next examined transcription of the DNA template on the nanoplatform during AFM scanning. We observed the formation of a "stalled complex" when only three nucleotide triphosphates (ATP, CTP, and GTP in this experiment) were added.[10] A stalled complex can form between the template dsDNA and RNAP when UTP is absent, and the length of the short RNA transcript produced depends on the position of the first adenine after the T7 promoter. Using this template, RNAP stalled close to the T7 promoter region (Figure S7), position 3.21 ± 0.13 downstream ($n = 7$), which corresponds to the first position for U insertion. This shows that the arrested RNAP observed is a stalled complex. The complex was stable enough to maintain this structure for 14 s during AFM scanning. These results show that our system works for observation of transcription when the platform is adhered to the mica surface.

Finally, we examined the movement of the RNAP during transcription by high-speed AFM. In the presence of NTPs, we observed the RNAP movement from the promoter region and dissociation from the template dsDNA (Figure 5a and Movie S3). In a series of the reactions, single RNAP appeared around the promoter region (time = 2 s). The RNAP started to move downstream on the template dsDNA, with some visible products (time = 4–10 s), and continued to move toward the middle of the template dsDNA. Finally, RNAP dissociated from the dsDNA. In the expanded image (time = 6 s), a new product giving some unclear traces should be the RNA transcript synthesized from RNAP. Unstructured RNA is mobile during AFM scanning because of the flexibility of the RNA molecules. Therefore, the RNA molecules do not produce a clear image, which could depend on the length and AFM scanning speed. Previous biotinylated-RNA transcripts labeled with streptavidin produced similar images (Fig-

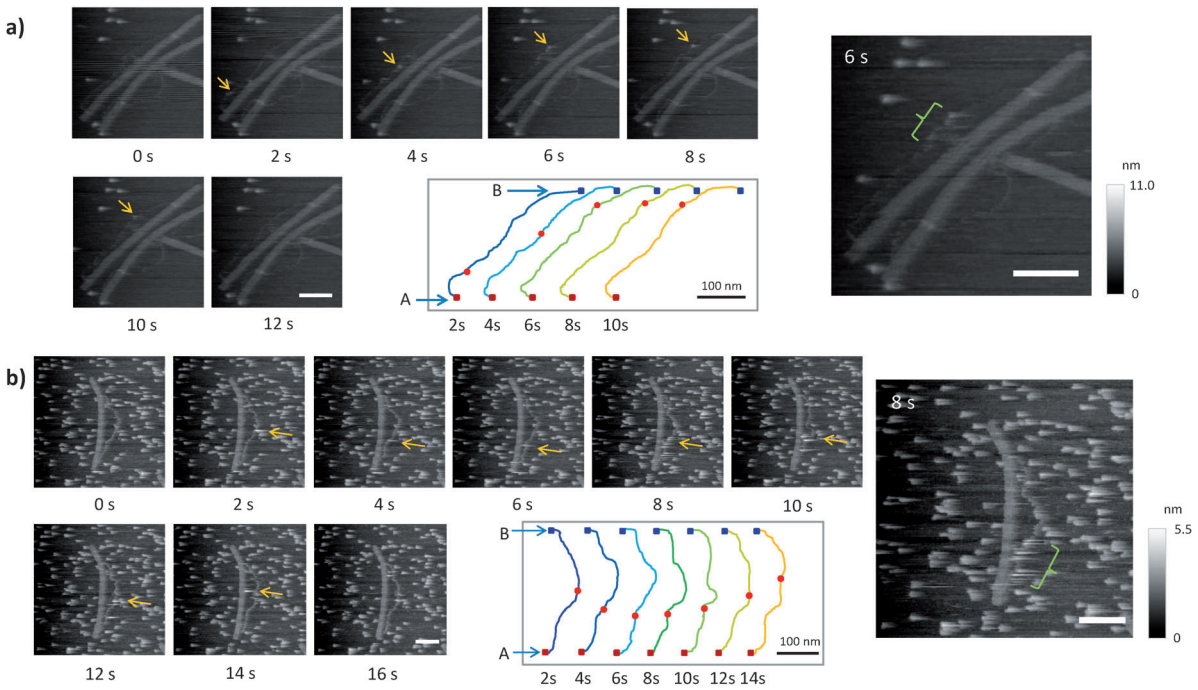

Figure 5. High-speed AFM images of transcription. Two different series of successive images are shown. NTP concentrations of a) 0.2 μM and b) 0.15 μM were used. Orange arrows = positions of RNAP. In the expanded images, unclear images of the RNA product (green) were observed during AFM imaging. Drawings of the shapes of the dsDNA chain and the positions of RNAP (red circle) are shown. Rectangles represent the positions of sites A (red) and B (purple) on the DNA nanoplatform. Scanning speed = 0.5 images s^{-1}. Scale bars = 100 nm.

ure S6). A similar phenomenon was also observed in the flexible movement of a dsDNA in which one end was not fixed.[22] The speed of the RNAP movement during transcription was not constant on the time-scale of the AFM measurement because of contact between the template dsDNA and the mica surface.

In addition, we obtained a series of images of transcription on the DNA nanoplatform, which showed binding to the template dsDNA, sliding on the template dsDNA, binding to the promoter region, RNA synthesis, and dissociation from the template dsDNA (Figure 5b and Movie S4). AFM images were acquired every two seconds. A single RNAP first attached to the middle of the template dsDNA (time = 2 s). The RNAP then slid upstream on the template dsDNA (time = 2–4 s) and stopped at the promoter region (time = 4–6 s). The RNAP started to move downstream, with some unclear traces (time = 8–12 s), and continued to move to the middle of the template dsDNA. Finally, the RNAP dissociated from the dsDNA (time = 14 s). At 8 s (expanded image on the right of Figure 5b), when RNAP transcription started, we again recorded some flexible products in the AFM image, which was completely different from the usual RNAP sliding. This could be the image of the synthesized RNA chain, similar to the flexible movement of the biotinylated RNA. RNAP dissociated without reaching the end of the template dsDNA, indicating that contact between the template dsDNA and the mica surface may prevent movement of RNAP and induce its detachment from the dsDNA. In addition, interaction of the AFM tip with dsDNA and RNAP may promote dissociation from the dsDNA.

In conclusion, we have demonstrated a novel method for direct observation of the behavior of RNAP using the designed nanoplatform and high-speed AFM imaging. We recorded the movement of a single T7 RNAP and transcription on a dsDNA at the molecular resolution allowed by the system. The template dsDNA attached to the platform was stable enough to be used for observation of the sliding of RNAP and transcription by RNAP. The shape of the dsDNA could be visualized because both ends of the dsDNA were connected to the platform. The position of the RNAP on the dsDNA can be identified, and the displacement of the RNAP was easily measured. In addition, transcription occurred both in solution and on the mica surface using this system. A series of images of transcription, including binding, sliding, RNA synthesis, and dissociation was directly visualized. Our results show the first single-molecule imaging of RNA synthesis during transcription.

This tethered DNA system could be used for other DNA-binding proteins and enzymes that move along dsDNA during their reaction. In addition, the DNA nanostructure used herein is a useful platform for recording a number of detailed enzyme behaviors, including binding to DNA, searching for a specific sequence, catalyzing a reaction, and dissociating from DNA, at single-molecule resolution. This method could be extended to direct observation of various enzymatic phenomena in defined nanoscale spaces.

Received: March 9, 2012
Published online: July 29, 2012

Keywords: DNA origami · high-speed AFM · nanostructures · single-molecule experiments · transcription

[1] A. Engel, D. J. Müller, *Nat. Struct. Biol.* **2000**, *7*, 715 – 718.
[2] J. K. H. Hörber, M. J. Miles, *Science* **2003**, *302*, 1002 – 1005.
[3] W. A. Rees, R. W. Keller, J. P. Vesenka, G. Yang, C. Bustamante, *Science* **1993**, *260*, 1646 – 1649.
[4] M. Guthold, M. Bezanilla, D. A. Erie, B. Jenkins, H. G. Hansma, C. Bustamante, *Proc. Natl. Acad. Sci. USA* **1994**, *91*, 12927 – 12931.
[5] S. Kasas, N. H. Thomson, B. L. Smith, H. G. Hansma, X. Zhu, M. Guthold, C. Bustamante, E. T. Kool, M. Kashlev, P. K. Hansma, *Biochemistry* **1997**, *36*, 461 – 468.
[6] M. Guthold, C. Rivetti, G. Yang, N. H. Thomson, S. Kasas, H. G. Hansma, B. Smith, P. K. Hansma, C. Bustamante, *Biophys. J.* **1999**, *77*, 2284 – 2294.
[7] H. Kabata, O. Kurosawa, I. Arai, M. Washizu, S. A. Margarson, R. E. Glass, N. Shimamoto, *Science* **1993**, *262*, 1561 – 1563.
[8] R. J. Davenport, G. J. Wuite, R. Landick, C. Bustamante, *Science* **2000**, *287*, 2497 – 2500.
[9] J. H. Kim, R. G. Larson, *Nucleic Acids Res.* **2007**, *35*, 3848 – 3858.
[10] Y. Harada, O. Ohara, A. Takatsuki, H. Itoh, N. Shimamoto, K. Kinosita Jr., *Nature* **2001**, *409*, 113 – 115.
[11] T. Ando, N. Kodera, E. Takai, D. Maruyama, K. Saito, A. Toda, *Proc. Natl. Acad. Sci. USA* **2001**, *98*, 12468 – 12472.
[12] D. Yamamoto, T. Uchihashi, N. Kodera, H. Yamashita, S. Nishikori, T. Ogura, M. Shibata, T. Ando, *Methods Enzymol.* **2010**, *475*, 541 – 564.
[13] N. Kodera, D. Yamamoto, R. Ishikawa, T. Ando, *Nature* **2010**, *468*, 72 – 76.
[14] T. Uchihashi, R. Iino, T. Ando, H. Noji, *Science* **2011**, *333*, 755 – 758.
[15] P. W. K. Rothemund, *Nature* **2006**, *440*, 297 – 302.
[16] T. Tørring, N. V. Voigt, J. Nangreave, H. Yan, K. V. Gothelf, *Chem. Soc. Rev.* **2011**, *40*, 5636 – 5646.
[17] A. Rajendran, M. Endo, H. Sugiyama, *Angew. Chem.* **2012**, *124*, 898 – 915; *Angew. Chem. Int. Ed.* **2012**, *51*, 874 – 890.
[18] S. M. Douglas, H. Dietz, T. Liedl, B. Högberg, F. Graf, W. M. Shih, *Nature* **2009**, *459*, 414 – 418.
[19] H. Dietz, S. M. Douglas, W. M. Shih, *Science* **2009**, *325*, 725 – 730.
[20] S. M. Douglas, A. H. Marblestone, S. Teerapittayanon, A. Vazquez, G. M. Church, W. M. Shih, *Nucleic Acids Res.* **2009**, *37*, 5001 – 5006.
[21] M. Endo, Y. Katsuda, K. Hidaka, H. Sugiyama, *J. Am. Chem. Soc.* **2010**, *132*, 1592 – 1597.
[22] M. Endo, Y. Katsuda, K. Hidaka, H. Sugiyama, *Angew. Chem.* **2010**, *122*, 9602 – 9606; *Angew. Chem. Int. Ed.* **2010**, *49*, 9412 – 9416.
[23] Y. Sannohe, M. Endo, Y. Katsuda, K. Hidaka, H. Sugiyama, *J. Am. Chem. Soc.* **2010**, *132*, 16311 – 16313.

